Applied Physics Express 6 (2013) 127002
http://dx.doi.org/10.7567/APEX.6.127002

Light-Immune pH Sensor with SiC-Based Electrolyte–Insulator–Semiconductor Structure

Yi-Ting Lin[1], Chien-Shiang Huang[1], Lee Chow[2], Jyun-Ming Lan[1], Chia-Ming Yang[3,4], Liann-Be Chang[4,5]*, and Chao-Sung Lai[1,4]*

[1]*Department of Electronic Engineering, Chang Gung University, Kweishan, Taoyuan 333, Taiwan*
[2]*Department of Physics, University of Central Florida, Orlando, FL32816, U.S.A.*
[3]*Institute of Electro-optical Engineering, Chang Gung University, Kweishan, Taoyuan 333, Taiwan*
[4]*Biosensor Group, Biomedical Engineering Research Center, Chang Gung University, Kweishan, Taoyuan 333, Taiwan*
[5]*Green Technology Research Center, Chang Gung University, Kweishan, Taoyuan 333, Taiwan*
E-mail: liann@mail.cgu.edu.tw; cslai@mail.cgu.edu.tw

Received August 19, 2013; accepted October 23, 2013; published online November 15, 2013

An electrolyte–insulator–semiconductor (EIS) structure with high-band-gap semiconductor of silicon carbide is demonstrated as a pH sensor in this report. Two different sensing membranes, i.e., gadolinium oxide (Gd_2O_3) and hafnium oxide (HfO_2), were investigated. The HfO_2 film deposited by atomic layer deposition (ALD) at low temperature shows high pH sensing properties with a sensitivity of 52.35 mV/pH and a low signal of 4.95 mV due to light interference. The EIS structures with silicon carbide can provide better visible light immunity due to its high band gap that allows pH detection in an outdoor environment without degradation of pH sensitivity.

Electrical detection of chemical and biological species through microelectronic devices, such as ion-sensitive field-effect transistor (ISFET),[1)] light-addressable potentiometic sensor (LAPS),[2)] and organic thin-film transistors (OTFTs),[3)] have attracted renewed attentions in the past decades. Among these semiconductor-based sensors, ISFET was first proposed with the sensing membrane of silicon dioxide (SiO_2) in 1970. The ISFET has advantages of small size, low cost, fast response time, and high durability over the conventional ion selective electrode (ISE)[4)] for (bio-)chemical applications. An electrical signal difference is generated by charged molecules at the electrolyte surface on the sensing membrane and following the modulation of channel current of the sensors. The operating mechanism is similar to that of the conventional metal–oxide–semiconductor field-effect transistor (MOSFET).[5)]

To obtain good sensing performance, many dielectric materials such as tantalum oxide (Ta_2O_5),[6)] zin oxide (ZnO),[7)] aluminum oxide (Al_2O_3),[8)] and titanium oxide (TiO_2)[9)] were investigated as sensing materials for pH detection. For the compatibility and integration with CMOS technology, an ion-sensitive membrane without silicon oxide (SiO_2) buffer layer has been proposed for pH detection using high-k material. Among numerous proposed high-k oxides, gadolinium oxide (Gd_2O_3)[10)] and hafnium oxide (HfO_2)[11)] have been proposed as an alternative gate dielectric with a wide band gap, good thermal stability and a relatively large conduction band offset. Recently, HfO_2 and Gd_2O_3 as a highly sensitive bio-field-effect device (bioFET) for biomedical detection using capacitance–voltage (C–V) measurement.[10,11)] Through the high-band-gap material, the light transmits to silicon bulk and generates electron–hole pairs in the silicon bulk. The light penetration leads to the shift of the threshold voltage dependence on the intensity of incident light.[12)] The effect of light penetration is a serious drawback that limits the ISFET applications to certain illuminated environments. In order to improve the situation, Gimmel et al.[13)] and Liao et al.[14)] used a metal layer as a light shelter to increase photoimmunity. The light effect was improved effectively but an additional complication remains. In contrast with Si-ISFETs, the diamond electrolyte-solution-gate field effect transistor (SGFET) was first introduced by Kawarada.[15)] The SGEFTs show the higher light-immunity because diamond has a wide band gap of 5.5 eV and is almost free of allowed electronic state between the valence and conduction band edges.[16)] However, the sensitivity of 42–48 mV/pH of SGEFT with different surface plasma treatments is lower as compared with that of high-k ISFET.

Wide-band-gap semiconductors are appealing devices due to several features such as thermal stability and high breakdown voltage. Much of the recent attention has been given to silicon carbide (SiC), which is the most mature material of the wide-band-gap (2.0–7.0 eV) semiconductors. SiC is an attractive semiconducting material owing to its unique electronic properties, mechanical robustness, chemical inertness, non-toxicity and biocompatibility.[17–21)] It holds a great sensing potential when applied to in-vitro biosensors, biologically interfaced neural networks, and intelligent implantable medical devices. Several conjugation techniques have been developed for the attachment of specific biomolecules to the SiC surface through the various cross-linking molecules.[22–25)]

In this work, SiC is used to replace silicon substrate as a supporting layer of the electrolyte–insulator–semiconductor (EIS) capacitive sensor. The EIS structure is one of the simplest platforms to replace ISFET in this preliminary investigation of the properties of new sensing structures. The new sensing properties we investigated include high pH sensitivity and high light immunity.

All EIS samples are separated into two groups for this systematic study. The process flow diagrams for both groups are summarized in Fig. 1(a). The first group is fabricated on p-type silicon substrate with Gd_2O_3 and HfO_2 sensing membrane. After the standard RCA cleaning, the Gd_2O_3 and HfO_2 layers are deposited directly on the silicon wafer by means of e-beam evaporator and atomic layer deposition (ALD) system. In comparison with the first group, the second one is composed with the same structure using the same oxide sensing layers except for the substrate which is replaced by silicon carbide wafer. The thicknesses of the Gd_2O_3 and HfO_2 layers in both groups are 30 and 10 nm, respectively. Following oxide deposition, a 300-nm-thick aluminum (Al) film was evaporated on the backside contact region of the wafer after removing the native oxide. The sensing area was defined by photolithography with a negative photoresist SU-8 2005 (Micro Chem.), which is also used as

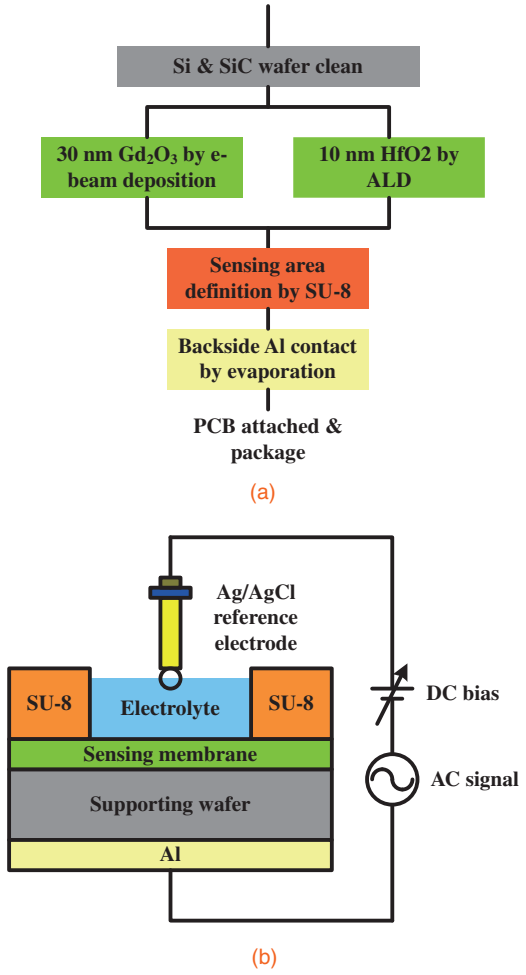

Fig. 1. (a) Fabrication process and (b) schematic of cross section of EIS structures.

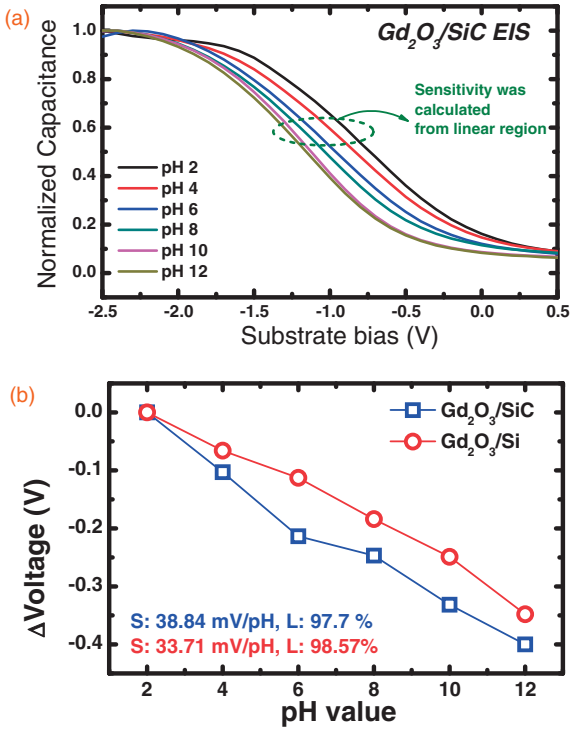

Fig. 2. (a) Typical C–V curves of Gd_2O_3/Si EIS structure for buffer solution of various pHs. (b) The pH sensitivity and linearity fitting from response voltage in various buffer solutions.

a waterproof layer. The radius of the sensing area exposed to the electrolyte was 2 mm. The wafer is diced into chips of $0.6 \times 0.6\,cm^2$. The EIS samples are assembled with silver gel on a printed circuit board (PCB). To prevent the leakage of electrolyte through wafer to the conductive metal pad, an epoxy was used to encapsulate the EIS structure and PCB. The EIS structure with a high-k sensing dielectric is the same for both groups in this study and is shown schematically in Fig. 1(b).

The investigation of pH-sensing properties is carried out in a standard buffer solution (Merck) from pH 2 to 12. All buffer solutions were checked after the experiment to ensure that the pH of the buffer solution does not change significantly during the experiment. In order to stabilize the surface reaction, all EIS samples were immersed in a reserve osmosis (RO) water for 12 h before the experiment. The electrical characterization of the EIS sensor was performed by means of the C–V method using an Aglient HP4284A high-precision LCR meter. The EIS sensor was immersed in the buffer solution with a Ag/AgCl reference electrode. To minimize high-frequency noise and noises due to light, all measurements were carried out in a Faraday cage at room temperature (25 °C). Each EIS sample was measured 3 times for accuracy of data extraction.

The typical C–V curves of Gd_2O_3/Si and Gd_2O_3/SiC EIS measured at various pHs from 2 to 12 are shown in Fig. 2(a). The normalized C–V curves were shifted to positive bias as the hydrogen ion concentration increased. The flat-band voltage shift was calculated at 0.6 of the maximum capacitance (C_{max}) of the C–V curves. The pH sensitivity was quantified by the linear fitting of the reference voltage. The pH sensitivity and linearity are plotted in Fig. 2(b). We found that the pH sensitivities of Gd_2O_3/Si EIS and Gd_2O_3/SiC EIS are 33.71 and 38.83 mV/pH, respectively. The theoretical sensitivity of EIS is 59 mV/pH at room temperature (25 °C) from the Nernst equation. The EIS devices with an e-beam-deposited Gd_2O_3 layer on top of the Si or SiC semiconductor substrate with a little porous due to physical deposition and have a lower pH sensitivity than ideal case. Because of the sensing membrane was directly deposited on the substrate without buffer SiO_2 layer. The gate leakage current passed through and into the substrate. Moreover, the Gd_2O_3 membrane was corroded after acid/base immersion resulted in a more porous structure. It could be resulted in hydration and degradation of Gd_2O_3 surface. Not only chemical resistance but also porous structure of Gd_2O_3 could both impacts on pH sensing properties. The stability of Gd_2O_3 can be improved by thermal-annealing after deposition.[26] These morphological changes may affect its sensitivity and durability. Compared with Gd_2O_3 membrane, the pH sensitivity of ALD-HfO_2 membrane can be effectively increased owing to dense, uniform, smooth, and conformal film deposition.

To further optimize the sensitivity of the EIS structure and to produce a high-quality thin film, the ALD system was used. The ALD system, allowing the possibility of dense, uniform, smooth and conformal thin film deposition, is an attractive method for thin-film preparation in CMOS technology. The response voltages in buffer solutions of various

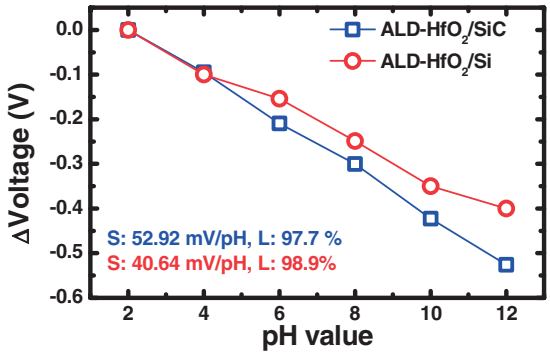

Fig. 3. The pH sensitivities and linearity of ALD-HfO_2/Si EIS and ALD-HfO_2/SiC EIS.

pHs with the ALD-HfO_2 thin-film was shown in Fig. 3. The pH sensitivity of ALD-HfO_2/Si EIS and ALD-HfO_2/SiC EIS were 40.64 and 52.92 mV/pH, respectively. The corresponding linearity is more than 99%. Compared with the e-beam-deposited Gd_2O_3 film, the high-quality ALD-HfO_2 film improves the hydrogen-ion-sensing properties of EIS structures. To summarize, both Gd_2O_3 and ALD-HfO_2 EIS structures with SiC substrate show higher pH sensitivity than the EIS structures with Si substrate. Since single-crystal SiC was grown by the solid-phase epitaxy method, there are more dangling bonds on the surface, which result in more electron traps at the interface between SiC and sensing oxide film. The negative traps attract more hydrogen ions to the sensing surface by electrostatic force, thus, a higher sensitivity was obtained.[27] In pH measurement, two interfering effects should be consider. One is related to the selectivity and the other is related to light response. For selectivity, pH response is almost up to 53 mV/pH for samples of SiC substrate. For this high sensitivity, the interfering effect is small. The other is light interfering effect of EIS structure.

Light immunity is crucial to the application of the pH sensor under different environments. In our previous study, the Ta_2O_5–SiO_2–Si EIS structures were also measured for light interfering effects. While the Ta_2O_5–SiO_2–Si EIS structures measured in the light condition, the raises were obtained on the C–V curves from the depletion region to inversion region. This phenomenon was obvious especially on the control sample without post-treatment.[26] In this study, the ALD-HfO_2 EIS structures with Si and SiC substrate are measured in the dark and under light exposure in order to study the issue of light response. The C–V curves obtained for ALD-HfO_2/SiC structures under dark or bright condition are shown in Fig. 4(a). As shown in the inset of Fig. 4(a), because of the wide-band-gap of SiC substrate, there are few voltage shifts from the depletion region to the inversion region. The light immunity of the ALD-HfO_2/Si structure compares poorly with ALD-HfO_2/SiC structure. Light-induced-current platform was used to detect directly the light response. With the design of light source matched to semiconductor band gap, photocurrent could be obtained by diffusion current generated ac signal in light source and revised bias in semiconductor. Therefore, the direct light immunity of Si and SiC EIS was investigated based on same confirm the light immunity as shown in Fig. 4(a). Then spectrum of laser diode was analyzed by LAB-LMS-100

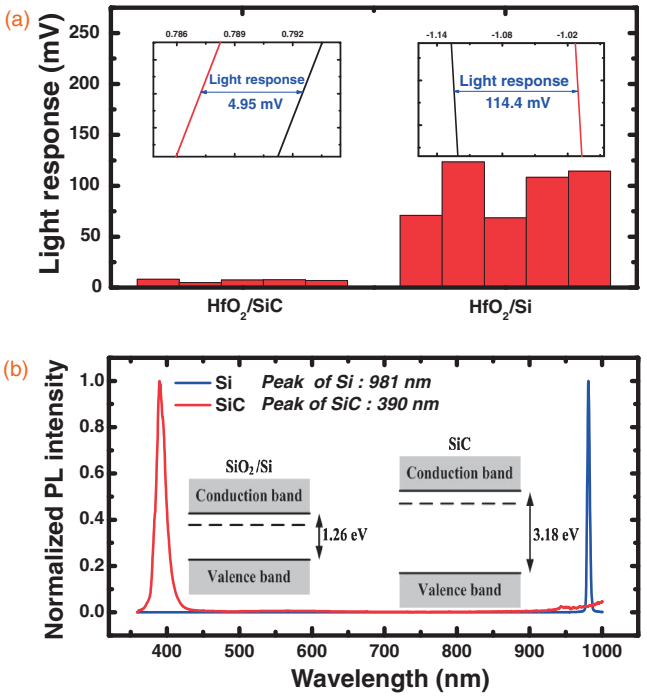

Fig. 4. (a) Histograms of ALD-HfO_2/Si and ALD-HfO_2/SiC EIS light exposure conditions. (b) The spectrum of laser diode.

Table I. Sensing properties of Gd_2O_3/Si, ALD-HfO_2/Si, and ALD-HfO_2/SiC EIS structures obtained from C–V measurement.

Wafer material	Membrane		
	Gd_2O_3	ALD-HfO_2	
	Sens. (mV/pH)	Sens. (mV/pH)	Light response (mV)
Si	27.4 ± 5.6	40.04 ± 1.31	97.14 ± 25.6
SiC	34.9 ± 4.8	52.35 ± 0.62	7.05 ± 1.2

light measurement spheres. The relationship between band gap and wavelengths can be written as $E = 1240/\lambda$. For Si, we thus obtain a band gap of 1.26 eV at 981 nm, and for SiC, a band gap of 3.18 eV at 390 nm. Due to high-band-gap material of HfO_2, the light can penetrate the HfO_2 film into the Si substrate to generate electron–hole pairs that causes the reference voltage to shift and, therefore, it was difficult to accomplish an accurate analysis. In contrast with the Si substrate, the SiC substrate with its high-energy band gap shows higher light immunity due to its ability to prevent electron–hole pair generation when sample was measured in light environment. The measured EIS parameters are summarized in Table I.

In this study, the wide-band-gap material, SiC, was investigated in the EIS structure for pH sensing application for the first time. The average pH sensitivity of 52.35 mV/pH is obtained from the SiC-based EIS with an ALD-HfO_2 sensing membrane. Under light exposure condition, the SiC substrate is an attractive candidate with a low light response (3.9–8.6 mV) due to its intrinsic property of having a wide band gap.

Acknowledgments This work was supported by the National Science Council, R.O.C. and Chang Gung University under contract Nos. NSC-101-2221-E-182-034-MY3 and UERPD2B0271, and by Chang Gung Memorial Hospital CMRPD1C0031, respectively.

1) P. Bergveld: IEEE Trans. Biomed. Eng. **17** (1970) 70.
2) J. H. Yang, T. F. Lu, J. C. Wang, C. M. Yang, D. G. Pijanowska, C. H. Chin, C. E. Lue, and C. S. Lai: Sens. Actuators B **180** (2013) 71.
3) M. E. Roberts, S. C. B. Mannsfeld, R. M. Stoltenberg, and Z. Bao: Org. Electron. **10** (2009) 377.
4) C. S. Lai, T. F. Lu, C. M. Yang, Y. C. Lin, D. G. Pijanowska, and B. Jaroszewicz: Sens. Actuators B **143** (2010) 494.
5) C. S. Lee, S. K. Kim, and M. Kim: Sensors **9** (2009) 7111.
6) C. S. Lai, C. E. Lue, C. M. Yang, J. H. Jao, and C. C. Tai: Sens. Actuators B **130** (2008) 77.
7) M. Spijkman, E. C. P. Smits, K. F. M. Chillessen, F. Biscarini, P. W. M. Bolm, and D. N. de Leeuw: Appl. Phys. Lett. **98** (2011) 043502.
8) H. J. Jang, T. E. Bae, and W. J. Cho: Appl. Phys. Lett. **100** (2012) 253703.
9) H.-J. Jang, J.-G. Gu, and W.-J. Cho: Sens. Actuators B **181** (2013) 880.
10) M. H. Wu, H. W. Yang, M. Y. Hua, Y. B. Peng, and T. M. Pan: Biosens. Bioelectron. **47** (2013) 99.
11) I.-S. Wang, Y.-T. Lin, C.-H. Huang, T.-F. Lu, C.-E. Lue, P. Yang, D. G. Pijanswska, C.-M. Yang, J.-C. Wang, J.-S. Yu, Y.-S. Chang, C. Chou, and C.-S. Lai: Nanoscale Res. Lett. **7** (2012) 179.
12) C.-L. Wu, J.-C. Chou, W.-Y. Chung, T.-P. Sun, and S.-K. Hsiung: Mater. Chem. Phys. **63** (2000) 153.
13) P. Gimmel, K. D. Schierbaum, W. Göpel, H. H. van den Vlekkert, and N. F. de Rooij: Sens. Actuators B **1** (1990) 345.
14) H. K. Liao, C. L. Wu, J. C. Chou, W. Y. Chung, T. P. Sun, and S. K. Hsiung: Sens. Actuators B **61** (1999) 1.
15) H. Kawarada, Y. Araki, T. Sakai, T. Ogawa, and H. Umezawa: Phys. Status Solidi A **185** (2001) 79.
16) Y. Sasaki and H. Kawarada: J. Phys. D **43** (2010) 374020.
17) J. B. Casady and R. W. Johnson: Solid-State Electron. **39** (1996) 1409.
18) A. Lemmon, M. Mazzola, J. Gafford, and C. Parker: IEEE Trans. Power Electron. **28** (2013) 4453.
19) S. Hertel, D. Waldmann, J. Jobst, A. Albert, M. Albrecht, S. Reshanov, A. Schöner, M. Krieger, and H. B. Weber: Nat. Commun. **3** (2012) 957.
20) N. Komatsu, T. Satoh, M. Honjo, T. Futatuki, K. Masumoto, C. Kimura, and H. Aoki: Appl. Surf. Sci. **257** (2011) 8307.
21) K. G. Menon, A. Nakajima, L. Ngwendson, and E. M. S. Narayanan: IEEE Electron Device Lett. **32** (2011) 1272.
22) R. Yakimova, R. M. Petoral, G. R. Yazdi, C. Vahlberg, A. Lloyd Spetz, and K. Uvdal: J. Phys. D **40** (2007) 6435.
23) A. L. Spetz, S. Nakagomi, H. Wingbrant, M. Andersson, A. Salomonsson, S. Roy, G. Wingqvist, I. Katardjiev, M. Eickhoff, K. Uvdal, and R. Yakimova: Mater. Manuf. Process. **21** (2006) 253.
24) A. Oliveros, A. Guiseppi-Elie, and S. E. Saddow: Biomed. Microdevices **15** (2013) 353.
25) E. H. Williams, A. V. Davydov, A. Motayed, S. G. Sundaresan, P. Bocchini, L. J. Richter, G. Stan, K. Steffens, R. Zangmeister, J. A. Schreifels, and M. V. Rao: Appl. Surf. Sci. **258** (2012) 6056.
26) C. E. Lue, T. C. Yu, C. M. Yang, D. G. Pijanowska, and C. S. Lai: Sensors **11** (2011) 4562.
27) T. F. Lu, J. C. Wang, C. S. Lai, C. M. Yang, M. H. Wu, C. P. Liu, R. S. Huang, and Y. C. Fan: IEDM Tech. Dig., 2009, p. 603.